



VL-Uncertainty: Detecting Hallucination in Large Vision-Language Model via Uncertainty Estimation

Ruiyang Zhang¹ Hu Zhang² Zhedong Zheng^{1*}

¹ FST and ICI, University of Macau, China

² CSIRO Data61, Australia

<https://github.com/Ruiyang-061X/VL-Uncertainty>

Abstract

Given the higher information load processed by large vision-language models (LVLMs) compared to single-modal LLMs, detecting LVLM hallucinations requires more human and time expense, and thus rise a wider safety concerns. In this paper, we introduce VL-Uncertainty, the first uncertainty-based framework for detecting hallucinations in LVLMs. Different from most existing methods that require ground-truth or pseudo annotations, VL-Uncertainty utilizes uncertainty as an intrinsic metric. We measure uncertainty by analyzing the prediction variance across semantically equivalent but perturbed prompts, including visual and textual data. When LVLMs are highly confident, they provide consistent responses to semantically equivalent queries. However, when uncertain, the responses of the target LVLM become more random. Considering semantically similar answers with different wordings, we cluster LVLM responses based on their semantic content and then calculate the cluster distribution entropy as the uncertainty measure to detect hallucination. Our extensive experiments on 10 LVLMs across four benchmarks, covering both free-form and multi-choice tasks, show that VL-Uncertainty significantly outperforms strong baseline methods in hallucination detection.

1. Introduction

Large vision-language models (LVLMs), capable of perceiving the world through diverse modalities, e.g., text, and images, have been widely applied in fields, e.g., medical diagnosis [15, 25, 38], embodied robotic [17, 26, 39], and autonomous driving [8, 45, 50]. Despite their impressive performance, similar to large language models (LLMs) [18, 18], LVLMs inevitably generate hallucination with over confidence, if any, posing serious risks in safety-

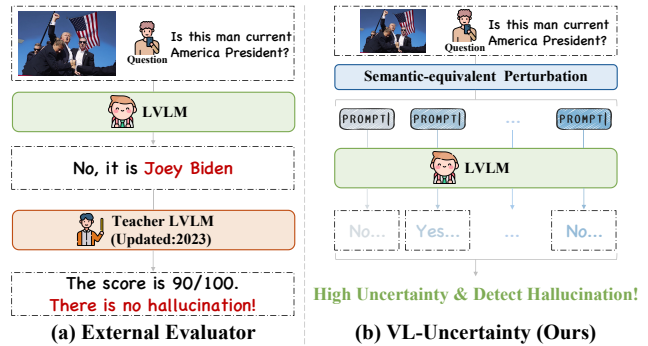


Figure 1. **Our motivation.** External evaluator-based methods usually suffer from knowledge missing when it comes to new domains (see (a)). In contrast, our VL-Uncertainty elicits intrinsic uncertainty of LVLM through proposed semantic-equivalent perturbation. Finally, refined uncertainty estimation facilitates reliable LVLM hallucination detection (see (b)).

critical scenarios [2, 31]. Compared to single-modal LLMs, detecting hallucination in LVLMs demands a deep understanding of multiple modalities [41]. It not only poses the challenges of the question understanding, but also the difficulty in checking the answer authenticity. Therefore, researchers have resorted to the automatic hallucination detection.

Most existing works for LVLM hallucination detection are based on external knowledge sources [28, 44, 54]. These methods can be coarsely divided into two families. One line of approaches [19, 49] utilizes manually annotated ground truth, such as parsed real-world facts from knowledge databases [44], to verify whether the responses of LVLMs are hallucinatory. Another line of methods relies on the pseudo annotations from extra models [28, 47]. For instance, some works introduce a ‘teacher-student’ paradigm [54]. The teacher LVLM takes the original question and the student answer as input and then scores the student answer. The student answers rating with low scores indicate hallucinations. In real-world scenarios, we, how-

*Correspondence to zhedongzheng@um.edu.mo.

ever, usually meet brand new problems, such as the impact of breaking news. We could apply the LVLM to give a prediction, but we do not know the probability of the hallucination. Both hallucination detection methods tend to fail, since we do not have the ground-truth reference, but we also can not rely on the out-of-the-date teacher LVLMs (see Fig. 1).

In an attempt to address this challenge, we propose VL-Uncertainty, the first uncertainty-based framework tailored for LVLM hallucination detection. Distinct from prior approaches that necessitate auxiliary information, our method intrinsically quantifies the uncertainty inherent to LVLM answers, enabling a mechanism for autonomous validation. Upon identifying elevated levels of uncertainty within an LVLM response, VL-Uncertainty categorizes the response as potentially hallucinatory. Specifically, we implement a technique involving semantic-equivalent perturbations to the prompts, thereby evaluating the uncertainty via the dispersion observed in the resulting answers. The foundational premise guiding this approach is that, under conditions of high confidence, LVLMs exhibit a tendency to generate consistent responses to queries that are semantically equivalent. Conversely, if perturbations that alter prompt exterior presentation lead to a divergence with responses of model, high uncertainty or potential hallucination is indicated (see Fig. 2). In particular, we employ blurring as the semantic-inequivalent perturbation for visual prompts. Blurring maintains all elements of the original visual prompt and preserves underlying logic and meaning. This choice follows biological principles observed in the human visual system [3, 13] and simulates the effect of varying distances between visual signals and the retina. For textual prompts, we deploy an off-the-shelf LLM to perturb the question without altering its meaning. By adjusting the temperature of the LLM, we control the degree of perturbation, analogous to visual blurring. These visual and textual prompts, paired by their levels of perturbation, are then fed into the LVLM to obtain a series of answers. Considering multiple LVLM answers with different wording, we first cluster the predicted answers by their semantics and calculate the entropy of the cluster distribution to quantify LVLM uncertainty as a continuous scalar. The uncertainty yielded by the series of answers enables the identification of varying levels of hallucination without extra models or manual annotations. We conduct experiments with 10 LVLMs across 4 benchmarks, encompassing both free-form and multi-choice formats. Our results show that VL-Uncertainty consistently surpasses strong baselines by clear margin in LVLM hallucination detection. Further qualitative analysis validates the superiority of VL-Uncertainty in effectively capturing LVLM uncertainty, thereby facilitating accurate hallucination detection. In summary, our contributions are as follows:

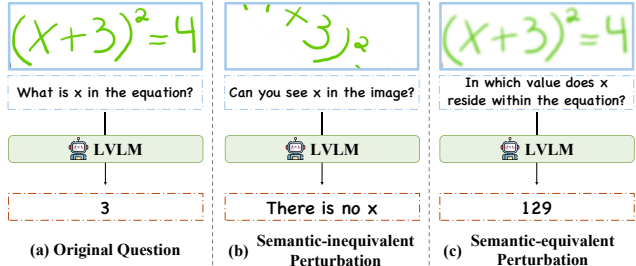


Figure 2. **Comparison between semantic-equivalent perturbations and inequivalent ones.** LVLMs inevitably generate hallucinatory answers (see (a)). While semantic-inequivalent perturbations yield correct answers, they do not provide insight into the uncertainty of LVLM for the original query, as shown in (b). In contrast, responses to semantically equivalent perturbed prompts, though potentially incorrect, offer valuable insight into the intrinsic uncertainty of LVLM. With only the exterior presentations of prompt altered, fluctuation of answers indicates elevated uncertainty (see (c)). This distinction highlights the utility of semantic-equivalent perturbations in assessing the reliability and consistency of LVLM responses.

- We propose a new uncertainty-based framework, VL-Uncertainty, for detecting hallucination in Multi-modal Large Language Models (LVLMs). We find that it is of importance to control the difficulty of prompts via semantic-equivalent perturbation, facilitating VL-Uncertainty capturing the randomness in LVLM response, indicating uncertainty and potential hallucination. Since it is an intrinsic metric, VL-Uncertainty could be easily scalable to new fields.
- We conduct extensive experiments on 10 LVLMs across 4 benchmarks, including both free-form and multi-choice tasks. Our results show that VL-Uncertainty outperforms strong baselines in LVLM hallucination detection, thereby enhancing the safety and reliability of LVLM applications.

2. Related Work

Large Vision-Language Models. Early works primarily focus on generating text responses based on image and text prompts [29, 30, 64]. Building on these foundational efforts, subsequent studies have significantly extended the capabilities and application domains of LVLMs [17, 53, 58]. Recent research has focused on refining prompt granularity from image-level to more detailed box- or point-level control [5, 58]. Based on these achievements, LVLMs have been applied in different fields, such as medical diagnosis [25, 38], embodied robotics [17, 39], and autonomous driving [8, 50]. While these developments enhance LVLM capabilities, complex cross-modal interactions are introduced, compromising response reliability. In high-stakes applications, unreliable LVLM responses present significant safety risks, leading to high demands for accurate

hallucination detection [15]. Distinct from existing approaches, we propose explicitly estimating intrinsic uncertainty of LVLM to facilitate hallucination detection, laying the foundation for safer human-LVLM interactions.

Uncertainty Learning. Uncertainty learning methods [12, 14] generally fall into three primary categories. (1) Single deterministic methods [35, 42, 62] modify a deterministic network to directly regress uncertainty. While these methods are straightforward and require minimal overhead, the predicted uncertainty, if no any regularization, has a potential to overfit all uncertain or very certain, compromising the training. (2) Bayesian methods [4, 10, 20, 51, 63] deploy stochastic Bayesian networks to quantify uncertainty by feeding the same input multiple times into one network with dynamic weights. Some works [10, 11, 37] leverages the dropout function, while others [6, 56] explicitly introduce Gaussian noise. The variance between different predictions quantifies the uncertainty. The primary challenge lies in modeling Bayesian networks in a computationally efficient way. Following the spirit, test-time augmentation [21, 33, 43, 46, 61] methods apply various augmentations to the input before feeding them to one single network. Similarly, variations in predictions due to these augmentations provide clues about uncertainty, though designing effective augmentations for meaningful uncertainty remains challenging. (3) Ensemble methods [16, 24, 36, 52] conduct inference on multiple deterministic networks for the same input, with the entropy of the ensemble group predictions estimating uncertainty. However, memory and computational costs increase significantly with more ensemble members. Diverging from these existing methods, we propose estimating LVLM uncertainty based on semantic-equivalent perturbation on vision-language prompts and variance of corresponding answer set.

LVLM Hallucination Detection. Research in this field can be divided into two main trajectories [2, 31]. (1) External-model-based evaluation: GAVIE [28] leverages strong LVLM as a smart teacher to score responses of student LVLMs, with low scores indicating hallucinations. However, reliance on external pseudo annotations limits its application in unknown domains. More recently, HaELM [47] specifically trains an LLM to score LVLM responses related to hallucinations. CCEval [60] suggests utilizing GPT4 API as intelligent parser to extract meaningful objects from responses and compare them with ground truth objects, although this introduces additional cost and resource. (2) Discrete rule-based checking: CHAIR [40] suggests utilizing the discrete ratio of objects presented in the answer relative to a ground-truth object list to identify hallucinatory responses. However, this approach is restricted to the 80 COCO object classes. Building on CHAIR, POPE [27] optimizes the prompting technique by focusing on Yes-or-No questions, simplifying the checking process and improving

evaluation stability. Unfortunately, treating hallucination detection purely as a binary classification task fails to capture the varying degrees of hallucinations. Distinct from existing works, our proposed uncertainty estimation is entirely self-contained and free of external knowledge, thereby offering greater flexibility and robustness. Moreover, we explicitly estimate uncertainty within LVLMs to continuously indicate different levels of hallucination.

3. Method

3.1. Semantic-equivalent Perturbation

Visual Prompts. Practically, we perturb the original input image multiple times by applying varying degrees of 2D Gaussian blurring (see Fig. 3). By adjusting blurring radius, we control the blur intensity from relatively clear to heavily blurred:

$$I_i = \phi_{\text{vis}}(I, r_i), \quad (1)$$

where I denotes the original visual prompt, r_i represents the radius of Gaussian blurring in the i -th perturbation, with $r_i < r_j$ for $i < j$. ϕ_{vis} refers to blurring operation and I_i is the i -th perturbed visual prompt. i ranges from 1 to N and N indicates the number of perturbations. Notably, blurring qualifies as a semantic-equivalent perturbation. It preserves the full content and structure of the original image, without introducing new objects or removing existing ones. This method maintains spatial information and the relationships between objects, given that it does not involve transformations like flipping or rotation. Visual attributes such as color, shape, and motion dynamics are also retained, ensuring the integrity of original image.

Textual Prompts. For textual prompts, we also employ semantic-equivalent perturbations by varying the wording, grammatical structure, and narrative style without altering the underlying meaning (see Fig. 3). To achieve this, we utilize a pre-trained text-only LLM, prompting it to rephrase the original question while preserving its semantics. Specifically, we design detailed LLM instruction that focuses on varying words, structure, and narrative, while ensuring semantic equivalence. During each perturbation, we adjust the temperature of utilized LLM to achieve varying degrees of alteration, analogous to the visual perturbations:

$$T_i = \phi_{\text{text}}(T, \tau_i), \quad (2)$$

where $i = 1, 2, \dots, N$, and N is the number of perturbation times. T represents the initial textual prompt, τ_i denotes the LLM temperature during the i -th perturbation, satisfying $\tau_i < \tau_j$ for $i < j$. ϕ_{text} refers to the utilized LLM and T_i is the i -th perturbed textual prompt.

Combination of Perturbed Prompts. We synchronize the perturbations of visual and textual prompts according to their respective degrees of perturbation. For visual

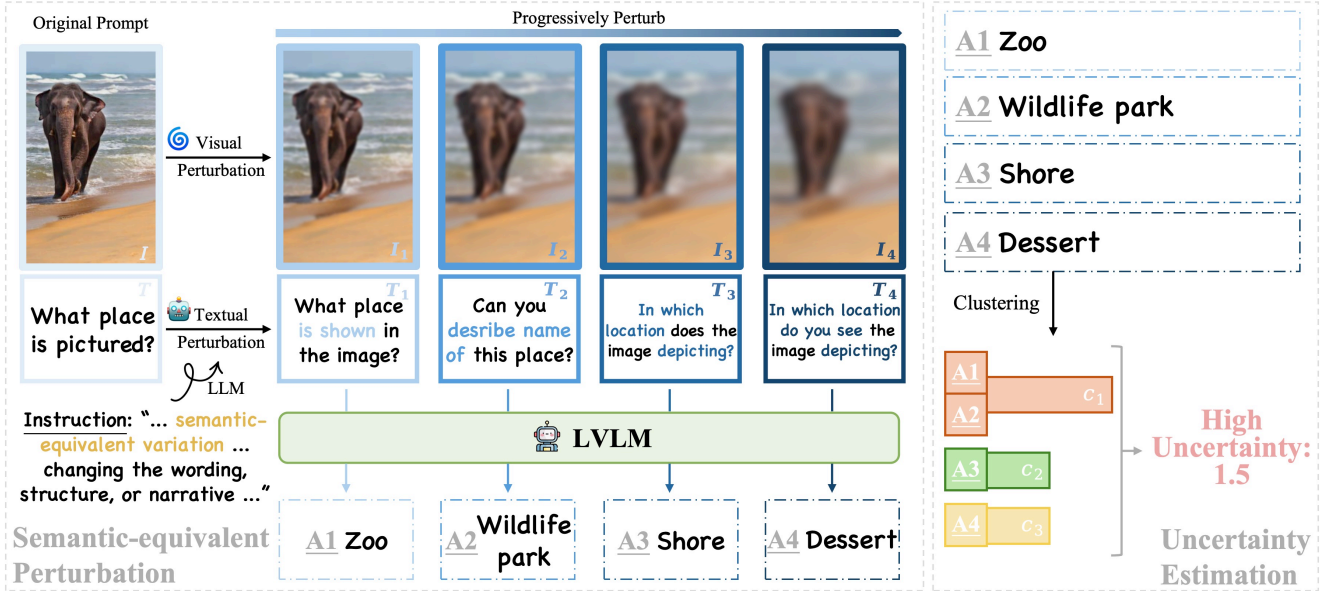


Figure 3. **Overall illustration of our proposed VL-Uncertainty.** To facilitate mining of uncertainty arising from various modalities, we apply semantic-equivalent perturbations (*left*) to both visual and textual prompts. For visual prompt, the original image is blurred to varying degrees, mimicking human visual perception. For textual prompt, pre-trained LLM is prompted to rephrase the original question in semantic-equivalent manner with different temperatures. Detailed instruction is designed to achieve question rephrasing with the original semantic preserved. Prompt pairs with varying degrees of perturbation are harnessed to effectively elicit LVLM uncertainty. We cluster LVLM answer set by semantic meaning and utilize entropy of answer cluster distribution as LVLM uncertainty (*right*). The estimated uncertainty serves as a continuous indicator of different levels of LVLM hallucination.

prompts, the degree is quantified by the blurring radius, where a larger radius indicates heavier blurring. For textual prompts, the degree is determined by the LLM temperature, with higher temperatures leading to more narrative variations. Each visual prompt is perturbed several times, from low to high degrees, and similarly, textual prompts undergo comparable degrees of perturbation. Finally, we pair visual prompts with textual prompts that have been perturbed to a similar extent $\{\langle I_i, T_i \rangle \mid i = 1, 2, \dots, N\}$, where I_i and T_i are the perturbed visual and textual prompts, respectively.

Discussion. Why is semantic-equivalent perturbation superior to semantic-inequivalent ones? Maintaining the original semantics of prompts during perturbation is essential. Semantically equivalent perturbation preserves the original meaning, ensuring that any fluctuations in responses stem directly from the inherent uncertainty of LVLM. This straightforward reflection of LVLM uncertainty enables more effective uncertainty estimation. In contrast, if perturbations alter prompt semantics, responses could reasonably change, while those variations could not reflect true uncertainty. This can misleadingly increase entropy and falsely suggest high uncertainty. For example, even if the LVLM has low uncertainty about a question, altering the meaning of prompt can lead to varied responses, incorrectly indicating high uncertainty. **What is the intuition behind utilizing image blurring?** We select typical *blurring* among various image perturbation techniques,

drawing inspiration from human visual perception [3, 13]. To illustrate this design, we take the nearsighted person as example. If their perception of an object remains stable regardless of whether they wear glasses, it indicates a low level of uncertainty about the object. Otherwise, it suggests a higher level of uncertainty about the object. Similarly, by applying varying degrees of blurring to visual prompts, we can measure the intrinsic uncertainty of LVLM: stable responses across different blur levels suggest low uncertainty, while significant changes in responses indicate higher uncertainty. Quantitative ablations further validate our intuition (see Table 2b).

3.2. Uncertainty Estimation

We quantify LVLM uncertainty by measuring the variance within the set of generated answers (see Fig. 3). Notably, we consider the entropy across different semantics rather than mere lexical variations. Specifically, we use a pre-trained LLM to evaluate mutual semantic entailment between pairs of LVLM answers. A pair of answers is considered semantically entailed only if each answer entails the other. This operation is iteratively applied across the entire set of sampled answers, grouping them by underlying meaning. We thus obtain a set of semantic clusters $\{c_i\}_{i=1}^{N_c}$, where N_c is the total number of semantic clusters with $N_c \leq N$. Then, we calculate the entropy of the cluster distribution to esti-

mate uncertainty:

$$U_{\text{LVLM}} = - \sum_{i=1}^{N_C} p(\mathbf{c}_i) \log p(\mathbf{c}_i), \quad (3)$$

where \mathbf{c}_i is the i -th semantic cluster containing answers with same semantics, $p(\mathbf{c}_i)$ denotes distribution probability of i -th semantic cluster. U_{LVLM} represents the estimated LVLM uncertainty.

Discussion. Why estimate uncertainty on answer variances against prompt perturbations, rather than allowing LVLMs to directly regress uncertainty like previous works [55]? We observe a severe over-confidence problem when allowing LVLMs to assign confidence scores to their own responses. For example, even with the prompt of hallucination, LVLM usually still regard their responses as absolutely correct and assign a high confidence score. This is similar to humans, *i.e.*, individuals tend to overestimate their confidence without repeated consideration [22, 34]. To address this, we leverage prompt perturbations and multiple sampling to better capture LVLM uncertainty. By progressively perturbing prompts and sampling multiple times, we obtain a more refined uncertainty estimation. **What are benefits of VL-Uncertainty over vanilla semantic entropy [9, 23]?** VL-Uncertainty is tailored for vision-language scenarios with semantically equivalent perturbations for each modality. The semantically equivalent perturbations enable fine-grained reflection of the LVLM on the given prompts. Additionally, the design of the image-text pairs is with increasing perturbations. Compared with the relatively random temperature design in [9, 23], the proposed method contains different levels of difficulty in the prompts of both modalities.

3.3. LVLM Hallucination Detection

Notably, our estimated uncertainty is continuous and proficient in indicating varying levels of hallucination, from minor deviations to complete logical incoherence. This continuous measure effectively captures the full spectrum of hallucinations encountered in LVLMs. However, existing benchmarks lack such continuous, fine-grained ground truth. To obtain quantitative results and compare with previous methods, we establish a decision threshold for our estimated uncertainty: answers with uncertainty exceeding this threshold are predicted as hallucinatory, while those below it are considered not. Finally, we compare hallucination detection predictions with the hallucination ground truth labels to assess the accuracy of VL-Uncertainty in detecting hallucinations as $(N_{\text{F-N}} + N_{\text{T-P}}) / N_{\text{Total}}$, where $N_{\text{F-N}}$ (False-Negative) refers to count of cases where answer is hallucinatory and VL-Uncertainty predict the answer as hallucinatory, $N_{\text{T-P}}$ (True-Positive) refers to count of cases where answer is non-hallucinatory and VL-Uncertainty predict the

answer as non-hallucinatory. N_{Total} is the total number of questions. This metric indicates the proportion of correct predictions (both hallucinatory and non-hallucinatory) made by VL-Uncertainty across all evaluated cases.

Discussion. Can VL-Uncertainty be applied to any LVLM in the image-text domain? VL-Uncertainty is a versatile and scalable hallucination detection framework that can be applied to any image-text LVLM. It leverages both the input prompts and output answers of LVLMs to enable effective uncertainty estimation and hallucination detection, regardless of the specific structure or design of the LVLMs. As a result, VL-Uncertainty offers greater flexibility and robustness.

4. Experiment

Benchmarks. Our experiments utilize both multi-choice and free-form benchmarks. For multi-choice benchmarks, we employ MMMU [59] and ScienceQA [32]. MMMU presents a challenging set of college-level multi-modal questions spanning 30 subjects with 11.5K questions. ScienceQA comprises quiz questions typically found in American high school curricula, covering subjects like physics, chemistry, and biology, with a total of 21,208 samples split into training (12,726), validation (4,241), and testing set (4,241). For free-form benchmarks, we utilize MM-Vet [57] and LLaVA-Bench [30], which include questions and answers in varied formats and lengths. MM-Vet, a recent benchmark, evaluates integrated LVLM capabilities across 6 basic abilities and 16 combinations, with 218 free-form question samples that span a range of topics. LLaVA-Bench, pioneering in assessing higher-level LVLM capabilities like logical reasoning, contains 60 distinct questions categorized into ‘convention’, ‘detail’, and ‘complexity’.

LVLMs. We experiment with 10 LVLMs from 4 distinct model groups. Specifically, we utilize LLaVA1.5 [30], LLaVA-NeXT [29], Qwen2VL [48], and InternVL2 [7]. LLaVA1.5 introduces visual instruction tuning. It aligns a pre-trained vision encoder with an LLM through a projection layer and enables simultaneous processing of image and text. LLaVA-NeXT scales up the baseline model with richer data sources to enhance reasoning, video understanding, and world knowledge capabilities. Qwen2VL overcomes the limitations of predefined image resolution and enables LVLMs to handle various resolutions. InternVL2 focuses on scaling up the vision encoder within the alignment pipeline to improve general visual-language abilities.

Implementation Details. We implement a unified codebase for LVLM uncertainty estimation and hallucination detection by including adopted benchmarks, LVLMs, baselines, and our VL-Uncertainty. Detailed settings for our VL-Uncertainty are as follows: (1) Initial answer generation. We set a low temperature of 0.1 for all LVLMs. The generated answer is compared with benchmark label to ob-

MM-Vet	Qwen2VL-2B	Qwen2VL-7B	Qwen2VL-72B	LLaVA1.5-7B	LLaVA1.5-13B	InternVL2-1B	InternVL2-8B	InternVL2-26B	LLaVANEXT-7B	LLaVANEXT-13B
GAVIE [28]	29.36	43.58	51.38	23.39	24.77	30.73	30.73	22.48	37.61	43.58
Semantic Entropy [9]	60.55	57.80	62.84	72.48	79.36	72.94	55.05	58.72	61.01	72.48
VL-Uncertainty (ours)	69.72	64.22	71.56	82.11	80.28	74.31	65.14	64.22	72.02	74.31
LLaVA-Bench	Qwen2VL-2B	Qwen2VL-7B	Qwen2VL-72B	LLaVA1.5-7B	LLaVA1.5-13B	InternVL2-1B	InternVL2-8B	InternVL2-26B	LLaVANEXT-7B	LLaVANEXT-13B
GAVIE [28]	25.00	26.67	40.00	15.00	20.00	30.00	31.67	31.67	45.00	35.00
Semantic Entropy [9]	61.67	55.00	61.67	70.00	70.00	65.00	60.00	53.33	61.67	65.00
VL-Uncertainty (ours)	70.00	68.33	71.67	83.33	78.33	71.67	66.67	73.33	68.33	68.33
MMMU	Qwen2VL-2B	Qwen2VL-7B	Qwen2VL-72B	LLaVA1.5-7B	LLaVA1.5-13B	InternVL2-1B	InternVL2-8B	InternVL2-26B	LLaVANEXT-7B	LLaVANEXT-13B
GAVIE [28]	37.82	48.36	57.09	37.58	44.61	40.61	48.12	33.21	43.64	45.82
Semantic Entropy [9]	53.82	54.91	60.36	52.61	50.18	53.82	54.91	60.36	52.61	50.18
VL-Uncertainty (ours)	58.91	59.76	65.58	56.05	53.62	56.36	55.15	58.91	59.27	54.90
ScienceQA	Qwen2VL-2B	Qwen2VL-7B	Qwen2VL-72B	LLaVA1.5-7B	LLaVA1.5-13B	InternVL2-1B	InternVL2-8B	InternVL2-26B	LLaVANEXT-7B	LLaVANEXT-13B
GAVIE [28]	61.82	77.09	85.23	58.50	66.39	62.27	65.20	53.94	86.71	89.19
Semantic Entropy [9]	54.04	77.94	87.06	61.77	68.02	64.45	90.08	91.32	67.67	65.34
VL-Uncertainty (ours)	67.97	80.12	88.99	63.66	69.51	65.05	90.38	92.02	68.27	67.53

Table 1. Comparison with state-of-the-arts on both free-form benchmark (MM-Vet and LLaVABench) and multi-choice benchmark (MMMU and ScienceQA) for LVLm hallucination detection. Our VL-Uncertainty yields significant improvements over strong baselines. This validates the efficacy of our proposed semantic-equivalent perturbation in eliciting and estimating LVLm uncertainty more accurately, which further facilitates LVLm hallucination detection. The reported results are hallucination detection accuracy. We re-implement semantic entropy [9] within vision-language context.

tain whether this answer is hallucinatory. (2) Uncertainty estimation. We use a higher LVLm temperature to enable sampling process. In total, We perform 5 rounds of sampling. For visual perturbation, we employ 2D Gaussian blurring with radius in [0.6, 0.8, 1.0, 1.2, 1.4] to create different levels of image blur. For textual perturbation, we use a small LLM, Qwen2.5-3B-Instruct [1], to rephrase questions, applying temperatures of [0.1, 0.2, 0.3, 0.4, 0.5]. The prompt for rephrasing is ‘Given the input question, generate a semantically equivalent variation by changing the wording, structure, grammar, or narrative. Ensure the perturbed question maintains the same meaning as the original.’. After we obtain sampled answer set, we use small LLM to check semantic entailment between answers. With answer set clustered by semantics, entropy of cluster distribution is calculated as uncertainty. (3) Hallucination detection. We utilize an uncertainty threshold of 1 for all experiments. If the estimated uncertainty is higher than the threshold, the initial answer is predicted by VL-Uncertainty as hallucination, while those lower are not. The hallucination predictions are compared with initial hallucination detection label (from (1)) to obtain hallucination detection accuracy. We utilize 2 H100 (80G) GPUs for all experiments. We also re-implement semantic-entropy [9] in the vision-language context since it is initially proposed in text-only domain.

4.1. Comparison with State-of-the-arts

We first present our hallucination detection results on the free-form question benchmarks (MM-Vet and LLaVABench) (see Table 1). Our VL-Uncertainty consistently achieves notable improvements over strong baselines [9, 23] across various LVLm architectures and model sizes. Specifically, we observe +10.09% for InternVL2-8B, +9.17% for Qwen2VL-2B, and +6.42% for Qwen2VL-7B on MM-Vet. These results validate the effectiveness of our proposed semantic-equivalent perturbation on both visual

and textual prompts in enhancing LVLm uncertainty estimation and thereby facilitating hallucination detection.

We also present our hallucination detection results on multi-choice benchmarks (ScienceQA and MMMU) in Table 1. The consistent improvements over strong baselines validate the robustness of VL-Uncertainty across various benchmarks. On ScienceQA, VL-Uncertainty outperforms baselines by clear margins within Qwen2VL [48] model group, achieving gains of +6.15%, +2.18%, and +1.93% for 2B, 7B, and 72B models, respectively. Furthermore, VL-Uncertainty achieves a high hallucination detection accuracy of 92.02% for InternVL2-26B, illustrating its substantial potential for effective hallucination detection.

4.2. Ablation Studies and Further Discussion

Separated visual and textual semantic-equivalent perturbation. We present the ablation results of our proposed semantic-equivalent perturbation in Table 2a. Single modality perturbation already yields substantial improvement compared to the vanilla baseline, with visual perturbation improving by +4.58% and textual perturbation by +1.83%. When semantic-equivalent perturbation is applied to both visual and textual prompts, VL-Uncertainty achieves optimal results with a performance of 82.11%, surpassing a strong baseline by a clear margin (+9.63%). This significant improvement validates the efficacy of our proposed perturbation approach in estimating LVLm uncertainty and enhancing LVLm hallucination detection.

Semantic-equivalent and inequivalent visual perturbations. We present a comparison between semantic-equivalent and semantic-inequivalent visual perturbations in Table 2b. Specifically, we implement several baselines: ‘Rotation’ rotates the original image with degrees in [-40, -20, 10, 20, 40]. ‘Flipping’ utilizes 2 horizontal flipped and 3 vertical flipped images. ‘Shifting’ moves the image up, down, left, and right within reasonable ranges. ‘Cropping’

(a)			(b)			(c)			(d)			(e)			(f)					
Visual Perturb.	Textual Perturb.	Hallu. Det. Acc.	Visual Perturb.	Equiva.	Acc.	Visual Perturb.	Equiva.	Acc.	Textual Perturb.	Sem. Equiva.	Hallu. Det. Acc.	Blurring Radius	Δ	Hallu. Det. Acc.	LLM Temperature	Δ	Hallu. Det. Acc.	LLM Structure	#Param.	Hallu. Det. Acc.
		72.48	Rotation	×	70.18	GaussianNoise	✓	73.85	Swapping	×	74.77	[0.1, 0.2, 0.3, 0.4, 0.5]	0.1	75.69	[0.01, 0.02, 0.03, 0.04, 0.05]	0.01	76.61	Qwen2.5-0.5B-Instruct	0.5B	50.92
✓		77.06	Flipping	×	71.56	Dropout	✓	73.85	Deleting	×	70.64	[0.6, 0.7, 0.8, 0.9, 1.0]	0.1	74.31	[0.05, 0.1, 0.15, 0.2, 0.25]	0.05	74.31	Qwen2.5-1.5B-Instruct	1.5B	69.27
	✓	74.31	Shifting	×	72.02	SaltAndPepper	✓	72.02	Inserting	×	67.43	[0.6, 0.8, 1.0, 1.2, 1.4]	0.2	82.11	[0.1, 0.2, 0.3, 0.4, 0.5]	0.1	82.11	Qwen2.5-3B-Instruct	3B	82.11
✓	✓	82.11	Cropping	×	67.43	Sharpen	✓	74.31	Replacing	×	71.56	[0.5, 1.0, 1.5, 2.0, 2.5]	0.5	76.15	[0.2, 0.4, 0.6, 0.8, 1.0]	0.2	78.44	Qwen2.5-7B-Instruct	7B	73.39
			Erasing	×	64.68	AdjustContrast	✓	71.56	LLM Rephrasing	✓	82.11				[0.4, 0.8, 1.2, 1.6, 2.0]	0.4	77.52			
			AdjustBrightness	✓	72.94	Blurring	✓	82.11												

Table 2. **Ablation studies on MM-Vet with LLaVA1.5-7B.** (a) Ablation study of semantic-equivalent perturbation design. Perturbations applied across both modalities (visual and textual) yield the best results. Notably, the interaction between perturbed visual and textual prompts enables effective mining of uncertainty in complex vision-language context, thereby facilitating more refined LLM hallucination detection. (b) Ablation study of semantic-equivalent and semantic-inequivalent visual perturbation. Semantic-equivalent visual perturbation, such as blurring, proves superior to all other semantic-inequivalent perturbations. This underscores the importance of preserving the original semantics of visual prompts during perturbation, which more effectively elicits LLM uncertainty. (c) Ablation study of semantic-equivalent and semantic-inequivalent textual perturbation. Among all textual perturbations, LLM rephrasing yields optimal results. Other rule-based perturbations fail to maintain the original semantics of textual prompts, resulting in unsatisfactory outcomes. (d) Ablation study of blurring radius in visual perturbation. Utilizing blurring radii of [0.6, 0.8, 1.0, 1.2, 1.4] for visual perturbations yields the best results. Radius with medium gap, such as 0.2, ensures a reasonable variance between perturbed visual prompts, thereby more effectively eliciting LLM uncertainty. (e) Ablation of LLM temperature in textual perturbation. LLM temperatures of [0.1, 0.2, 0.3, 0.4, 0.5] during perturbation yield the best results. This indicates that adjustments within a controlled range facilitate more effective elicitation of LLM uncertainty. (f) Ablation study of LLM for textual perturbation. Qwen2.5-3B-Instruct achieves best results among this LLM group.

adopts crop ratios in [0.95, 0.9, 0.85, 0.8, 0.75] regarding the original size. ‘Erasing’ randomly erases a square area with lengths in [50, 100, 150, 200, 250]. ‘GaussianNoise’ adds per-channel noise with scale in [0.05, 0.1, 0.15, 0.2, 0.25]. ‘Dropout’ randomly changes pixels to black with rate of [0.05, 0.1, 0.15, 0.2, 0.25]. ‘SaltAndPepper’ is similar to ‘Dropout’ but changes some pixels to white. ‘Sharpen’ enhances the original image with a degree in [0.1, 0.2, 0.3, 0.4, 0.5]. ‘AdjustBrightness’ and ‘AdjustContrast’ alter the corresponding property by a factor of [0.8, 0.9, 1.1, 1.2, 1.3]. Notably, Semantic-equivalent visual perturbation, such as blurring, yields optimal results by a clear margin. This confirms the effectiveness of preserving original visual semantics during perturbation. Conversely, semantic-inequivalent techniques, with actual semantics of visual prompt altered, typically result in unsatisfactory outcomes.

Semantic-equivalent and inequivalent textual perturbations. We further report an ablation study on comparing semantic-equivalent and inequivalent textual perturbations (see Table. 2b). For baselines: ‘Swapping’ randomly swaps two words in the question; ‘Deleting’ randomly deletes one word; ‘Inserting’ inserts one word at a random place; and ‘Replacing’ randomly changes one word with another. The observed pattern is similar to that in Table 2b: semantic-equivalent perturbations surpass the inequivalent ones by a clear margin. This confirms retaining the original semantics of textual prompts contributes to accurate uncertainty estimation and effective hallucination detection.

Design details of visual perturbation. We also report an

ablation study on design details for visual perturbation, focusing specifically on the blurring radius applied in different perturbations (see Table 2d). We observe that maintaining a reasonable variance between perturbed prompts is crucial for achieving better performance. In visual perturbation, a blurring radius gap of 0.2 yields the best results. Conversely, both excessively small and overly large radius gaps negatively impact performance. A minimal gap fails to provide a sufficient difference between perturbed visual prompts, limiting the effective mining of uncertainty in the visual modality. On the other hand, a large gap introduces excessive variance, leading to inflated uncertainty that hinders accurate LLM hallucination detection.

Design details of textual perturbation. We also present the ablation study on LLM temperature settings during textual perturbations in Table 2e. The best results from temperatures [0.1, 0.2, 0.3, 0.4, 0.5] for different perturbations, maintaining a medium temperature gap of 0.1. This pattern is similar to that observed in visual perturbations (see Table 2d), where a moderate gap yields the best results, both very small or large radius gaps compromise performance.

Choices of LLMs for textual perturbation. Additionally, we conduct the ablation study on LLMs in textual perturbation. We found that Qwen2.5-3B-Instruct is the optimal choice among models tested, as it balances the ability to generate semantically equivalent variations without introducing unrelated details. This model capacity is well-suited to maintaining semantic integrity in perturbed prompts, resulting in more accurate uncertainty estimation

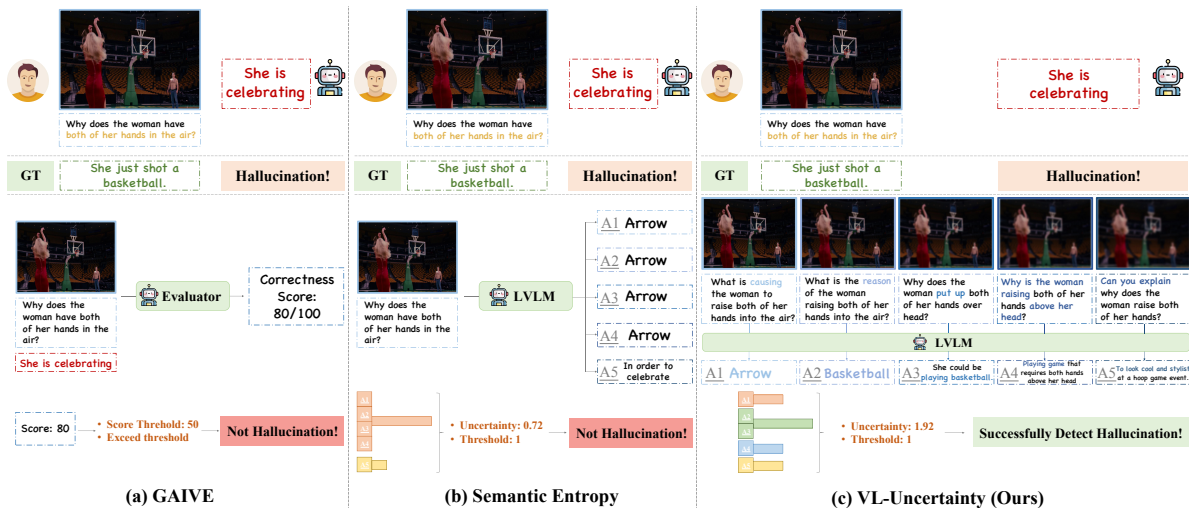


Figure 4. **Qualitative comparison between VL-Uncertainty and baselines.** We present a sample from free-form benchmark. For this hallucinatory sample, pseudo-annotation-based method [28] fails to interpret the hidden-behind logic and thus misses detecting hallucination (see (a)). On the other hand, for semantic-entropy [9], vanilla multi-sampling proves ineffective for mining LVLm uncertainty (see (b)). In contrast, our proposed semantic-equivalent perturbation on both visual and textual prompts successfully elicits LVLm uncertainty. This refined uncertainty estimation enhances the successful detection of LVLm hallucination (see (c)).

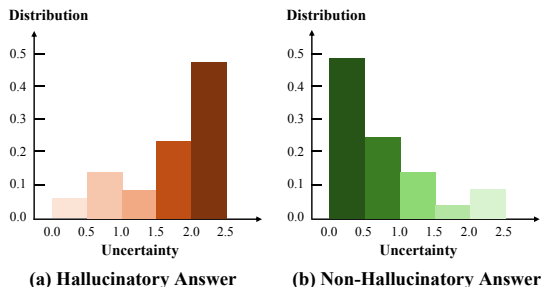


Figure 5. **Uncertainty distribution for hallucinatory and non-hallucinatory LVLm answers on MMVet.** Our VL-Uncertainty accurately assigns high uncertainty to hallucinatory answers and low uncertainty to non-hallucinatory answers. This distinct uncertainty distribution gap facilitates LVLm hallucination detection.

and improved hallucination detection. In contrast, smaller-capacity LLMs struggle to perform semantic-equivalent perturbation effectively on complex questions, degrading hallucination detection. Larger-capacity LLMs, on the other hand, tend to add unnecessary details to perturbed prompts, which hinders accurate uncertainty estimation.

4.3. Qualitative Analysis

We present a qualitative analysis comparing VL-Uncertainty with the vanilla baselines [9, 28] in Fig. 4. We present hallucinatory sample from free-form benchmarks. For GAVIE [28], external evaluator itself fails to interpret the underlying logic and thus misses detecting hallucination. In semantic entropy [9], simply increasing the temperature during uncertainty estimation is insufficient to effectively capture LVLm uncertainty. The LVLm consistently produces similar answers for hallucination cases, leading to inaccurate uncertainty estimation and suboptimal hallucination detection (see (b)). In contrast,

VL-Uncertainty, through our proposed semantic-equivalent perturbation, successfully captures high uncertainty and detects hallucinations in LVLms (see (c)).

Fig. 5 shows the statistical distribution of estimated uncertainty for hallucinatory and non-hallucinatory LVLm answers. Our estimated uncertainty closely calibrates with the accuracy of LVLm predictions: VL-Uncertainty predominantly assigns high uncertainty to hallucinatory answers, while assigning relatively low uncertainty to non-hallucinatory answers. The distinct gap in uncertainty distribution between hallucinatory and non-hallucinatory answers facilitates effective LVLm hallucination detection.

5. Conclusion

In this paper, we introduce VL-Uncertainty, the first uncertainty-based framework for detecting LVLm hallucinations. Distinct from existing approaches based on external knowledge, VL-Uncertainty harnesses LVLm uncertainty as an intrinsic metric to identify hallucination. Recognizing the complexities inherent in multi-modal contexts, we propose semantic-equivalent perturbations for both visual and textual prompts. For visual prompts, we apply blurring at different levels, inspired by human visual processing. For textual prompts, a pre-trained LLM rephrases questions without altering their semantic meaning. Pairs of perturbed prompts with varying perturbations are utilized to effectively elicit LVLm uncertainty. Variance of corresponding answer semantics is harnessed to quantify LVLm uncertainty. Notably, our uncertainty serves as a continuous indicator proficient in illustrating varying levels of LVLm hallucinations. Through experiments with 10 LVLms across 4 benchmarks (free-form and multi-choice), our VL-Uncertainty consistently demonstrates clear and substantial improvements over strong baselines, validating its effectiveness in LVLm hallucination detection.

References

- [1] Jinze Bai, Shuai Bai, Yunfei Chu, Zeyu Cui, Kai Dang, Xiaodong Deng, Yang Fan, Wenbin Ge, Yu Han, Fei Huang, et al. Qwen technical report. *arXiv*, 2023. 6
- [2] Zechen Bai, Pichao Wang, Tianjun Xiao, Tong He, Zongbo Han, Zheng Zhang, and Mike Zheng Shou. Hallucination of multimodal large language models: A survey. *arXiv*, 2024. 1, 3
- [3] Paul N Baird, Seang-Mei Saw, Carla Lanca, Jeremy A Guggenheim, Earl L Smith III, Xiangtian Zhou, Kyoko-Ohno Matsui, Pei-Chang Wu, Padmaja Sankaridurg, Audrey Chia, et al. Myopia. *Nature reviews Disease primers*, 6(1): 99, 2020. 2, 4
- [4] Charles Blundell, Julien Cornebise, Koray Kavukcuoglu, and Daan Wierstra. Weight uncertainty in neural network. In *ICML*, pages 1613–1622. PMLR, 2015. 3
- [5] Keqin Chen, Zhao Zhang, Weili Zeng, Richong Zhang, Feng Zhu, and Rui Zhao. Shikra: Unleashing multimodal llm’s referential dialogue magic. *arXiv:2306.15195*, 2023. 2
- [6] Yiyang Chen, Zhedong Zheng, Wei Ji, Leigang Qu, and Tat-Seng Chua. Composed image retrieval with text feedback via multi-grained uncertainty regularization. In *International Conference on Learning Representations (ICLR)*, 2024. 3
- [7] Zhe Chen, Jiannan Wu, Wenhai Wang, Weijie Su, Guo Chen, Sen Xing, Muyan Zhong, Qinglong Zhang, Xizhou Zhu, Lewei Lu, et al. Internvl: Scaling up vision foundation models and aligning for generic visual-linguistic tasks. In *CVPR*, pages 24185–24198, 2024. 5
- [8] Can Cui, Yunsheng Ma, Xu Cao, Wenqian Ye, Yang Zhou, Kaizhao Liang, Jintai Chen, Juanwu Lu, Zichong Yang, Kuei-Da Liao, et al. A survey on multimodal large language models for autonomous driving. In *WACV*, pages 958–979, 2024. 1, 2
- [9] Sebastian Farquhar, Jannik Kossen, Lorenz Kuhn, and Yarin Gal. Detecting hallucinations in large language models using semantic entropy. *Nature*, 630(8017):625–630, 2024. 5, 6, 8
- [10] Yarin Gal and Zoubin Ghahramani. Dropout as a bayesian approximation: Representing model uncertainty in deep learning. In *ICML*, pages 1050–1059. PMLR, 2016. 3
- [11] Yarin Gal, Jiri Hron, and Alex Kendall. Concrete dropout. *Advances in neural information processing systems*, 30, 2017. 3
- [12] Jakob Gawlikowski, Cedric Rovile Njéutcheu Tassi, Mohsin Ali, Jongseok Lee, Matthias Humt, Jianxiang Feng, Anna Kruspe, Rudolph Triebel, Peter Jung, Ribana Roscher, et al. A survey of uncertainty in deep neural networks. *Artificial Intelligence Review*, 56(Suppl 1):1513–1589, 2023. 3
- [13] Annechien EG Haarman, Clair A Enthoven, J Willem L Tideman, Milly S Tedja, Virginie JM Verhoeven, and Caroline CW Klaver. The complications of myopia: a review and meta-analysis. *Investigative ophthalmology & visual science*, 61(4):49–49, 2020. 2, 4
- [14] Wenchong He and Zhe Jiang. A survey on uncertainty quantification methods for deep neural networks: An uncertainty source perspective. *arXiv:2302.13425*, 2023. 3
- [15] Yutao Hu, Tianbin Li, Quanfeng Lu, Wenqi Shao, Junjun He, Yu Qiao, and Ping Luo. Omnimedvqa: A new large-scale comprehensive evaluation benchmark for medical lvlm. In *CVPR*, pages 22170–22183, 2024. 1, 3
- [16] Gao Huang, Yixuan Li, Geoff Pleiss, Zhuang Liu, John E Hopcroft, and Kilian Q Weinberger. Snapshot ensembles: Train 1, get m for free. *ICLR*, 2017. 3
- [17] Jiangyong Huang, Silong Yong, Xiaojian Ma, Xiongkun Linghu, Puhao Li, Yan Wang, Qing Li, Song-Chun Zhu, Baoxiong Jia, and Siyuan Huang. An embodied generalist agent in 3d world. *ICML*, 2024. 1, 2
- [18] Lei Huang, Weijiang Yu, Weitao Ma, Weihong Zhong, Zhangyin Feng, Haotian Wang, Qianglong Chen, Weihua Peng, Xiaocheng Feng, Bing Qin, et al. A survey on hallucination in large language models: Principles, taxonomy, challenges, and open questions. *arXiv*, 2023. 1
- [19] Liqiang Jing, Ruosen Li, Yunmo Chen, Mengzhao Jia, and Xinya Du. Faithscore: Evaluating hallucinations in large vision-language models. *EMNLP (Findings)*, 2024. 1
- [20] Alex Kendall and Yarin Gal. What uncertainties do we need in bayesian deep learning for computer vision? *NeurIPS*, 30, 2017. 3
- [21] Ildoo Kim, Younghoon Kim, and Sungwoong Kim. Learning loss for test-time augmentation. *NeurIPS*, 33:4163–4174, 2020. 3
- [22] Joshua Klayman, Jack B Soll, Claudia Gonzalez-Vallejo, and Sema Barlas. Overconfidence: It depends on how, what, and whom you ask. *Organizational behavior and human decision processes*, 79(3):216–247, 1999. 5
- [23] Lorenz Kuhn, Yarin Gal, and Sebastian Farquhar. Semantic uncertainty: Linguistic invariances for uncertainty estimation in natural language generation. *ICLR*, 2023. 5, 6
- [24] Balaji Lakshminarayanan, Alexander Pritzel, and Charles Blundell. Simple and scalable predictive uncertainty estimation using deep ensembles. *NeurIPS*, 30, 2017. 3
- [25] Chunyuan Li, Cliff Wong, Sheng Zhang, Naoto Usuyama, Haotian Liu, Jianwei Yang, Tristan Naumann, Hoifung Poon, and Jianfeng Gao. Llava-med: Training a large language-and-vision assistant for biomedicine in one day. *NeurIPS*, 36, 2024. 1, 2
- [26] Xiaoqi Li, Mingxu Zhang, Yiran Geng, Haoran Geng, Yuxing Long, Yan Shen, Renrui Zhang, Jiaming Liu, and Hao Dong. Manipllm: Embodied multimodal large language model for object-centric robotic manipulation. In *CVPR*, pages 18061–18070, 2024. 1
- [27] Yifan Li, Yifan Du, Kun Zhou, Jinpeng Wang, Wayne Xin Zhao, and Ji-Rong Wen. Evaluating object hallucination in large vision-language models. *EMNLP*, 2023. 3
- [28] Fuxiao Liu, Kevin Lin, Linjie Li, Jianfeng Wang, Yaser Yacoob, and Lijuan Wang. Mitigating hallucination in large multi-modal models via robust instruction tuning. In *ICLR*, 2024. 1, 3, 6, 8
- [29] Haotian Liu, Chunyuan Li, Yuheng Li, and Yong Jae Lee. Improved baselines with visual instruction tuning. In *CVPR*, pages 26296–26306, 2024. 2, 5
- [30] Haotian Liu, Chunyuan Li, Qingyang Wu, and Yong Jae Lee. Visual instruction tuning. *NeurIPS*, 36, 2024. 2, 5

- [31] Hanchao Liu, Wenyuan Xue, Yifei Chen, Dapeng Chen, Xiutian Zhao, Ke Wang, Liping Hou, Rongjun Li, and Wei Peng. A survey on hallucination in large vision-language models. *arXiv*, 2024. 1, 3
- [32] Pan Lu, Swaroop Mishra, Tanglin Xia, Liang Qiu, Kai-Wei Chang, Song-Chun Zhu, Oyvind Taffjord, Peter Clark, and Ashwin Kalyan. Learn to explain: Multimodal reasoning via thought chains for science question answering. *NeurIPS*, 35: 2507–2521, 2022. 5
- [33] Alexander Lyzhov, Yuliya Molchanova, Arsenii Ashukha, Dmitry Molchanov, and Dmitry Vetrov. Greedy policy search: A simple baseline for learnable test-time augmentation. In *Conference on uncertainty in artificial intelligence*, pages 1308–1317. PMLR, 2020. 3
- [34] Jan R Magnus and Anatoly A Peresetsky. Grade expectations: Rationality and overconfidence. *Frontiers in Psychology*, 8:2346, 2018. 5
- [35] Andrey Malinin and Mark Gales. Predictive uncertainty estimation via prior networks. *NeurIPS*, 31, 2018. 3
- [36] Andrey Malinin, Bruno Mlodozeniec, and Mark Gales. Ensemble distribution distillation. *arXiv:1905.00076*, 2019. 3
- [37] Dimity Miller, Lachlan Nicholson, Feras Dayoub, and Niko Sünderhauf. Dropout sampling for robust object detection in open-set conditions. In *2018 IEEE International Conference on Robotics and Automation (ICRA)*, pages 3243–3249. IEEE, 2018. 3
- [38] Michael Moor, Qian Huang, Shirley Wu, Michihiro Yasunaga, Yash Dalmia, Jure Leskovec, Cyril Zakka, Eduardo Pontes Reis, and Pranav Rajpurkar. Med-flamingo: a multimodal medical few-shot learner. In *Machine Learning for Health (MLH)*, pages 353–367. PMLR, 2023. 1, 2
- [39] Zhiliang Peng, Wenhui Wang, Li Dong, Yaru Hao, Shaohan Huang, Shuming Ma, and Furu Wei. Kosmos-2: Grounding multimodal large language models to the world. *ICLR*, 2024. 1, 2
- [40] Anna Rohrbach, Lisa Anne Hendricks, Kaylee Burns, Trevor Darrell, and Kate Saenko. Object hallucination in image captioning. *EMNLP*, 2018. 3
- [41] Pranab Sahoo, Prabhath Meharia, Akash Ghosh, Sriparna Saha, Vinija Jain, and Aman Chadha. A comprehensive survey of hallucination in large language, image, video and audio foundation models. *EMNLP (Findings)*, pages 11709–11724, 2024. 1
- [42] Murat Sensoy, Lance Kaplan, and Melih Kandemir. Evidential deep learning to quantify classification uncertainty. *NeurIPS*, 31, 2018. 3
- [43] Divya Shanmugam, Davis Blalock, Guha Balakrishnan, and John Guttag. Better aggregation in test-time augmentation. In *ICCV*, pages 1214–1223, 2021. 3
- [44] Zhiqing Sun, Sheng Shen, Shengcao Cao, Haotian Liu, Chunyuan Li, Yikang Shen, Chuang Gan, Liang-Yan Gui, Yu-Xiong Wang, Yiming Yang, et al. Aligning large multimodal models with factually augmented rlhf. *ACL (Findings)*, 2024. 1
- [45] Xiaoyu Tian, Junru Gu, Bailin Li, Yicheng Liu, Yang Wang, Zhiyong Zhao, Kun Zhan, Peng Jia, Xianpeng Lang, and Hang Zhao. Drivevlm: The convergence of autonomous driving and large vision-language models. *arXiv*, 2024. 1
- [46] Guotai Wang, Wenqi Li, Michael Aertsen, Jan Deprest, Sébastien Ourselin, and Tom Vercauteren. Aleatoric uncertainty estimation with test-time augmentation for medical image segmentation with convolutional neural networks. *Neurocomputing*, 338:34–45, 2019. 3
- [47] Junyang Wang, Yiyang Zhou, Guohai Xu, Pengcheng Shi, Chenlin Zhao, Haiyang Xu, Qinghao Ye, Ming Yan, Ji Zhang, Jihua Zhu, et al. Evaluation and analysis of hallucination in large vision-language models. *arXiv*, 2023. 1, 3
- [48] Peng Wang, Shuai Bai, Sinan Tan, Shijie Wang, Zhihao Fan, Jinze Bai, Keqin Chen, Xuejing Liu, Jialin Wang, Wenbin Ge, et al. Qwen2-vl: Enhancing vision-language model’s perception of the world at any resolution. *arXiv*, 2024. 5, 6
- [49] Shengkang Wang, Hongzhan Lin, Ziyang Luo, Zhen Ye, Guang Chen, and Jing Ma. Mfc-bench: Benchmarking multimodal fact-checking with large vision-language models. *arXiv*, 2024. 1
- [50] Wenhai Wang, Jiangwei Xie, ChuanYang Hu, Haoming Zou, Jianan Fan, Wenwen Tong, Yang Wen, Silei Wu, Hanming Deng, Zhiqi Li, et al. Drivemlm: Aligning multi-modal large language models with behavioral planning states for autonomous driving. *arXiv:2312.09245*, 2023. 1, 2
- [51] Max Welling and Yee W Teh. Bayesian learning via stochastic gradient langevin dynamics. In *ICML*, pages 681–688. Citeseer, 2011. 3
- [52] Yeming Wen, Dustin Tran, and Jimmy Ba. Batchensemble: an alternative approach to efficient ensemble and lifelong learning. *ICLR*, 2020. 3
- [53] Shengqiong Wu, Hao Fei, Leigang Qu, Wei Ji, and Tat-Seng Chua. Next-gpt: Any-to-any multimodal llm. *ICML*, 2024. 2
- [54] Wenyi Xiao, Ziwei Huang, Leilei Gan, Wangui He, Haoyuan Li, Zhelun Yu, Hao Jiang, Fei Wu, and Linchao Zhu. Detecting and mitigating hallucination in large vision language models via fine-grained ai feedback. *arXiv*, 2024. 1
- [55] Miao Xiong, Zhiyuan Hu, Xinyang Lu, Yifei Li, Jie Fu, Junxian He, and Bryan Hooi. Can llms express their uncertainty? an empirical evaluation of confidence elicitation in llms. *ICLR*, 2024. 5
- [56] Tianyuan Yu, Da Li, Yongxin Yang, Timothy M Hospedales, and Tao Xiang. Robust person re-identification by modelling feature uncertainty. In *Proceedings of the IEEE/CVF international conference on computer vision*, pages 552–561, 2019. 3
- [57] Weihao Yu, Zhengyuan Yang, Linjie Li, Jianfeng Wang, Kevin Lin, Zicheng Liu, Xinchao Wang, and Lijuan Wang. Mm-vet: Evaluating large multimodal models for integrated capabilities. *ICML*, 2024. 5
- [58] Yuqian Yuan, Wentong Li, Jian Liu, Dongqi Tang, Xinjie Luo, Chi Qin, Lei Zhang, and Jianke Zhu. Osprey: Pixel understanding with visual instruction tuning. In *CVPR*, pages 28202–28211, 2024. 2
- [59] Xiang Yue, Yuansheng Ni, Kai Zhang, Tianyu Zheng, Ruoqi Liu, Ge Zhang, Samuel Stevens, Dongfu Jiang, Weiming Ren, Yuxuan Sun, et al. Mmmu: A massive multi-discipline

- multimodal understanding and reasoning benchmark for expert agi. In *CVPR*, pages 9556–9567, 2024. 5
- [60] Bohan Zhai, Shijia Yang, Chenfeng Xu, Sheng Shen, Kurt Keutzer, and Manling Li. Halle-switch: Controlling object hallucination in large vision language models. page arXiv, 2023. 3
- [61] Guiyu Zhang, Huan-ang Gao, Zijian Jiang, Hao Zhao, and Zhedong Zheng. Ctrl-u: Robust conditional image generation via uncertainty-aware reward modeling. *arXiv*, 2024. 3
- [62] Ruiyang Zhang, Hu Zhang, Hang Yu, and Zhedong Zheng. Harnessing uncertainty-aware bounding boxes for unsupervised 3d object detection. *arXiv*, 2024. 3
- [63] Zhedong Zheng and Yi Yang. Rectifying pseudo label learning via uncertainty estimation for domain adaptive semantic segmentation. *International Journal of Computer Vision*, 129(4):1106–1120, 2021. 3
- [64] Deyao Zhu, Jun Chen, Xiaoqian Shen, Xiang Li, and Mohamed Elhoseiny. Minigt-4: Enhancing vision-language understanding with advanced large language models. *ICLR*, 2024. 2